POAC '99
Espoo, Finland

Proceedings of the 15th
International Conference on
Port and Ocean Engineering
under Arctic Conditions

MODEL ICE CLASS PROPELLER PERFORMANCE IN ICE OF VARIED STRENGTH

S. Searle[1], B. Veitch[2], and N. Bose[2]
[1]Oceanic Consulting Corporation, St. John's, Canada
[2]Memorial University of Newfoundland, St. John's, Canada

ABSTRACT

Experiments were done with a model ice-class propeller in an ice tank to investigate the variation of propeller performance with ice strength. The tests were designed to measure propeller shaft thrust and torque characteristics at varied values of the advance coefficient and compressive ice strength. The results are discussed in relation to a dimensional analysis of propeller thrust and torque measurements during ice interaction events. The implications for extrapolation of thrust and torque values to full-scale ice strengths are discussed.

1. INTRODUCTION

Work to update regulations for ice-class ships in a number of research groups around the world has resulted in, amongst other things, new methods for dimensioning ice-class propellers (e.g. Bose et al. 1998, Soininen et al. 1997, Katzmann and Andriushin 1997).

As part of an extended propeller-ice investigation looking at unconventional geometries and off design conditions, experiments were done in the ice tank at the Institute for Marine Dynamics (IMD), Canada, using two different propeller models. A model of the propeller on the passenger ferry *MV Caribou* was tested specifically to investigate the performance of a highly skewed propeller under ice loading over a range of operating and ice conditions. The model of a more conventional ice-class propeller from the Canadian *R-Class* icebreakers was tested over a wide range of operating and ice conditions to give loading characteristics in all four quadrants and an indication of performance at different ice strengths. This paper focuses on the question of how the ice loads of a propeller milling ice change as the ice strength varies. Results from the extended range of model propeller tests done under this program are described by Searle (1999).

2. TEST EQUIPMENT AND FACILITIES

The propeller used was a 200mm diameter model of the 4.12 meter diameter fixed pitch propeller fitted to the Canadian *R-Class* icebreakers. This propeller model was used for previous experimental programs investigating the propeller-ice interaction problem (e.g. Walker, 1996, Doucet, 1996). The *R-Class* propeller characteristics are given in Table 1 and a photo of the model is shown in Figure 1. The model was fitted to a propeller boat, as shown in Figure 2, and the propeller boat was fitted to the tow carriage in the IMD Ice Tank. EG/AD/S model ice (Timco, 1986) was used in the experimental program. The ice sheet used was approximately 60mm thick and had target compressive strengths of 60kPa to 90kPa. The test equipment and the instrumentation are described in detail by Searle et al. (1999).

Table 1: *R-Class* model particulars.

Number of Blades	4
Diameter, *D*	0.200 m
Pitch ratio, *P/D*	0.779
EAR	0.670

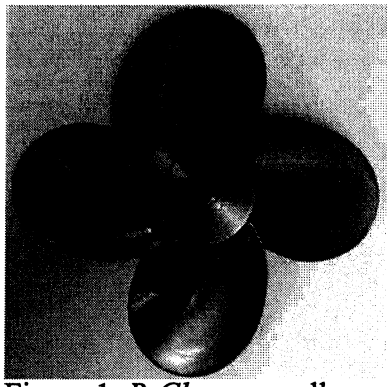

Figure 1. *R-Class* propeller model.

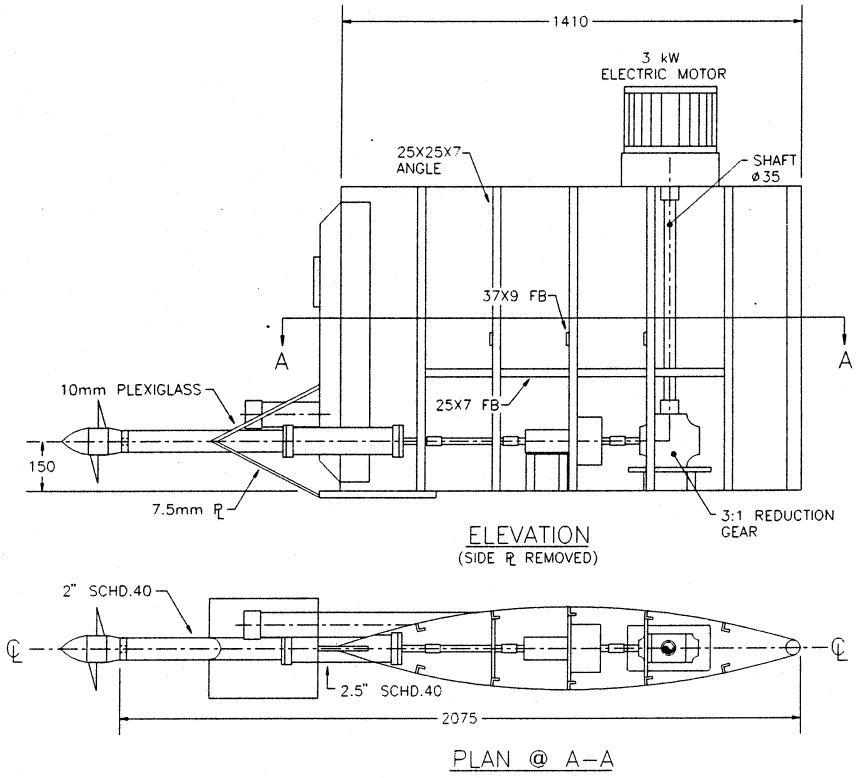

Figure 2. Schematic of propeller boat.

3. TEST PROGRAM

The tests involved setting up the model propeller to mill the underside of a stationary level ice sheet, which was floating on the water surface of the tank. The propeller boat was attached to the ice tank carriage in such a way that it could be moved vertically, enabling the propeller to be positioned at a predetermined depth relative to the ice sheet. Once at the correct position, the propeller boat was driven into the ice sheet edge and the propeller milled its underside. To limit the amount of ice used, a pre-sawn pattern of rectangles, each measuring approximately 0.5m×0.5m, was cut in the ice sheet prior to each run. The saw cuts were only about half way through the ice thickness so that the sheet did not lift vertically during cutting, but did break easily as the propeller boat penetrated the ice sheet.

The frictional torque in the shaft bearings was measured by conducting regularly scheduled friction tests: i.e. by measuring torque loading with a dummy hub equal to the mass of the propeller fitted in place of the propeller.

The test program for the quadrant 1 operations presented in this paper (forward propeller rotation at forward speeds of advance) was subdivided into three sets of experiments to investigate the relationship between thrust and torque loads, advance coefficient, and ice strength. Each of the test series was conducted at a nominal cut depth, h_I, of 25mm (h_I/D =0.125) while the advance coefficient was varied between 0.1 and 1.0. The shaft speed was 9rps for all tests. The test matrix for the three series is shown in Table 2, where the values of h_I and S_C are measurements, rather than targets.

The three series of tests were conducted at different ice strengths: 91kPa, 66kPa and 58kPa, respectively. Each individual test series was completed in a short time period to ensure that the time dependent ice properties were constant for the test conditions in that series. A relatively long time interval between series was used to temper the ice so that consecutive series were tested at decreasing values of compressive ice strengths. Samples were cut from the ice sheet throughout the test program and compressive strength test specimens were prepared from the samples. Each strength test specimen was a rectangular prism measuring 60×60×180mm. Uniaxial compressive strength was measured perpendicular to the columnar grains in a compression test machine. Each of the values given in the tables is an interpolated value of 3 or more measurements of compressive strength made immediately before, during and after the corresponding tests.

Table 2: Test matrix.

Variable	Series 1	Series 2	Series 3
J	0.1 to 1.0 step 0.05	0.1 to 1.0 step 0.1	0.1 to 1.0 step 0.2
h_I (mm)	24	25	24
S_C (kPa)	91	66	58

The following non-dimensional coefficients are used to present the data: advance coefficient, thrust coefficient, torque coefficient, a depth of cut coefficient, and a compressive ice strength index respectively:

$$J = \frac{V_A}{nD} \quad (1)$$

$$K_T = \frac{T}{\rho_w n^2 D^4} \quad (2)$$

$$K_Q = \frac{Q}{\rho_w n^2 D^5} \quad (3)$$

$$\lambda_d = \frac{h_I}{D} \quad (4)$$

$$K_S = \frac{S_C}{\rho_I n^2 D^2} \quad (5)$$

In these, V_A is the speed of advance of the propeller, which is equal to the carriage speed; n is the shaft rotational speed; D is the propeller diameter; ρ_W and ρ_I are the densities of water and ice; h_I is the depth of cut into the ice; T is the propeller thrust; Q is the propeller torque, and S_C is the uniaxial compressive strength of the ice.

4. EXPERIMENTAL RESULTS AND DISCUSSION

The time series for a portion of the milling period during a run at $J = 0.3$, and $S_C = 91$kPa is shown in Figure 3, where approximately seventy consecutive blade passes through the ice can be detected. The sampling rate was 5,000 Hz. The variability in the loads is likely due to local flexing in the ice sheet as it was milled. In addition to the time history, the probability density histograms of the thrust and torque loads for this run are shown in Figure 4. For each test run, the maximum and minimum values were determined and 50 evenly spaced cell ranges were constructed between the extreme data points.

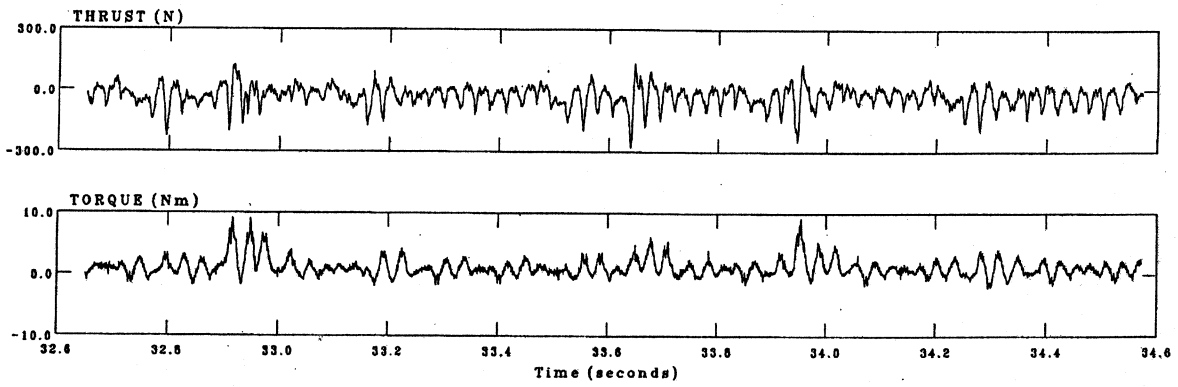

Figure 3. Time series ($J = 0.3$ and $S_C = 91$ kPa).

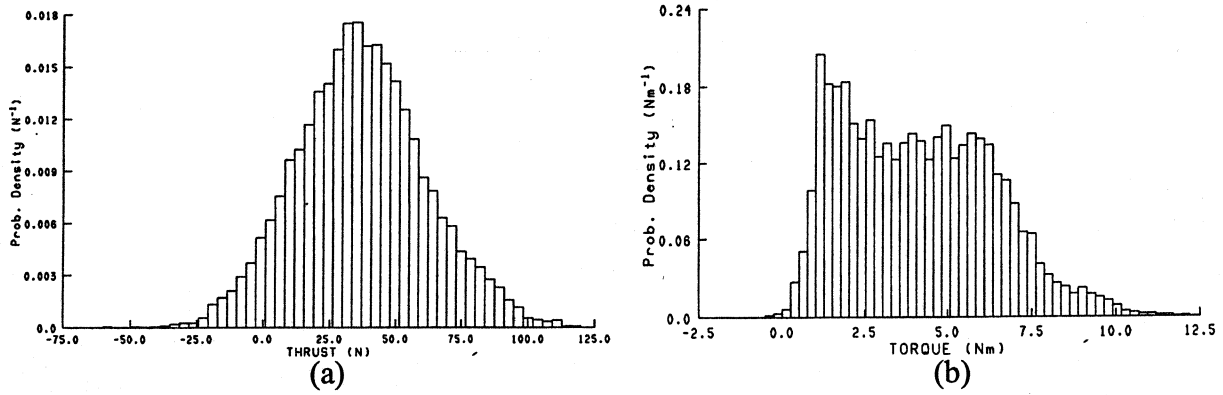

Figure 4. Thrust and torque distributions ($J = 0.3$ and $S_C = 91$ kPa).

Figure 4a shows that the shaft thrust distribution is close to normally distributed. The same type of distribution was found to occur for the majority of the runs while the range of distribution was dependent on the absolute magnitude of the loads measured: the larger the loads, the larger the range. For low values of torque, the distribution behaved in a similar manner to the thrust. For runs, like that shown in Figure 4b, where the torque loads were relatively high, the torque distribution was more broadly spread and showed a tendency towards a double peaked distribution. This was possibly a result of two primary torque peaks resulting from hydrodynamic loads and ice contact loads.

4.1 Variations in advance coefficient

The cut depth was held constant while the propeller was run the length of the ice tank over a range of advance coefficient, which was changed by holding the shaft speed constant at 9rps and changing the advance speed of the propeller. The results for each value of compressive strength (91kPa, 66kPa and 58kPa) are presented in Figures 5 to 7. The solid black circles are the experimental means for the thrust and torque coefficients and the solid line through these points are lines of best fit. The open circles are the maximum values measured during the test program, the open triangles are the minimum values, and the lines through each of these data sets are lines of best fit for the maximum and minimum thrust and torque coefficients. In addition, the open water performance curves are plotted on the applicable charts for reference. Each of the lines fitted through the data is modelled by a 3rd order polynomial.

With reference to Figures 5(a) to 7(a), the mean K_T increases as J increases from its minimum value up to $J \approx 0.2$ to 0.3, where the maximum mean K_T occurs. As J increases further, the mean K_T diminishes gradually. For all three ice strengths tested, the mean K_T during ice milling was greater than the open water K_T for advance coefficients less than about 0.5 or 0.6, and less than the open water K_T for higher J. The point at which the mean measured thrust drops below the open water thrust marks the transition of the net resultant thrust component of ice load from forward acting to backward acting. For the portions of the mean load curves that are above the open water curves, the resultant load acts on the pressure side of the blade, which causes an increase in both the total thrust and torque loads. When the mean K_T curve intersects the open water curve the resultant force acts close to the leading edge of the blade, such that there is a torque component to the contact load, but the mean thrust component is, on average, insignificant and the total thrust load consists of only the hydrodynamic component. As advance coefficient increases above this point, the resultant force moves back along the suction side of the blade creating at first a negative thrust component combined with a positive torque component. Eventually the resultant force shifts far enough along the suction side that both the thrust and torque components go negative.

With respect to the maximum and minimum thrust measurements, the worst loads are those that act on the suction side of the blades at high J and result in negative K_T values of -1 to -2.5. Open water thrust for this propeller goes to zero at $J \approx 0.9$, so in practice, the propeller would not operate at the highest J values shown in the figures. The type of interaction geometry that these conditions represent could be encountered during transitory operations, such as ice ridge ramming cycles, and the corresponding high backward loads might be a concern for propeller blade strength.

With respect to the results shown in each of Figures 5(b) to 7(b), the mean K_Q increases as J increases from its minimum value up to $J \approx 0.3$ to 0.4, where the maximum mean K_Q occurs. As J increases further, K_Q diminishes gradually and eventually drops below the open water K_Q (at $J \approx 1.0$, 0.85, and 0.75 for $S_C = 91$, 66, and 58 kPa respectively). At the point that the measured mean K_Q drops below the open water K_Q, the propeller is no longer acting as a propulsor.

As far as the propeller strength is concerned, the highest loads are the maximums that occur at $J \approx 0.4$, where the net resultant ice load acts near the leading edge and contributes to a positive thrust on the propeller. Ice strength has a marked influence on the maximum K_Q load.

In addition, the experiments indicated that the thrust and torque loads for the *R-Class* propeller are highly oscillatory. The thrust load displayed maximum and minimum loads with approximately equal components to either side of the mean load, while the torque displayed unequal components to either side of the mean, with the maximum component being the larger.

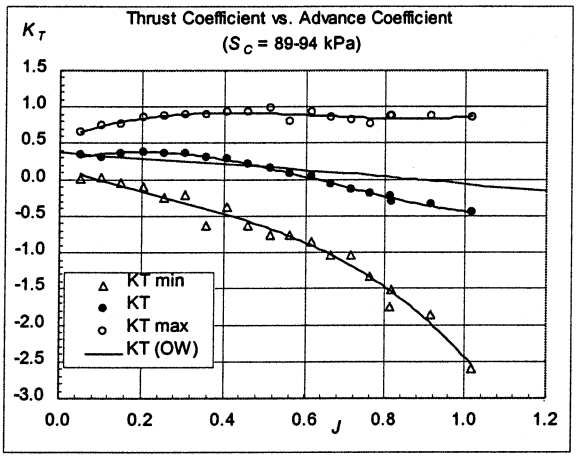

(a)

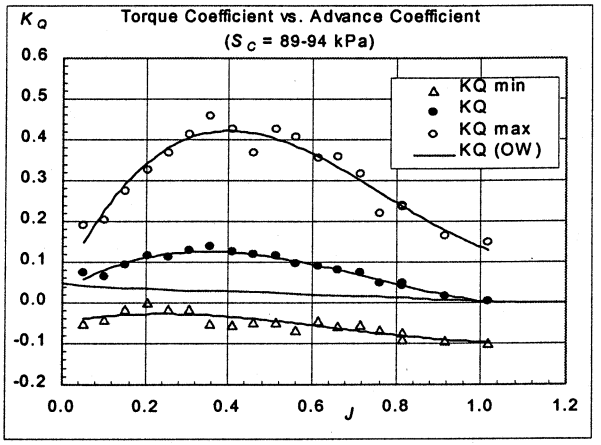

(b)

Figure 5. K_T and K_Q versus J for the *R-Class* propeller (S_C = 91 kPa).

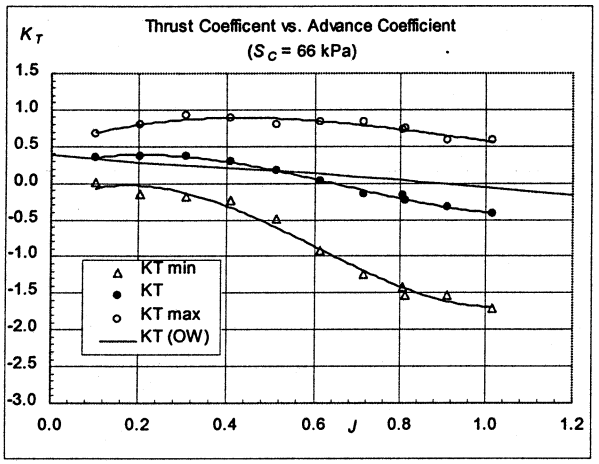

(a)

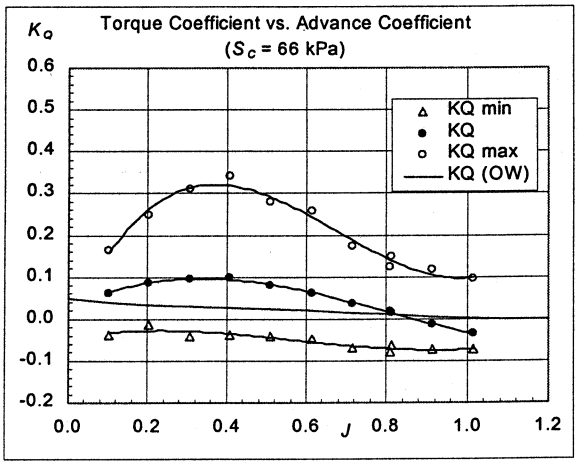

(b)

Figure 6. K_T and K_Q versus J for the *R-Class* propeller (S_C = 66 kPa).

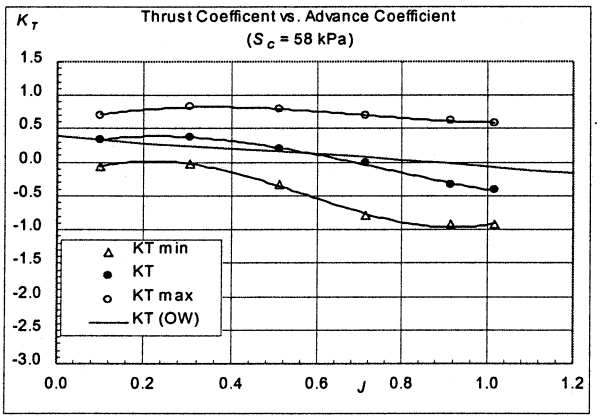

(a)

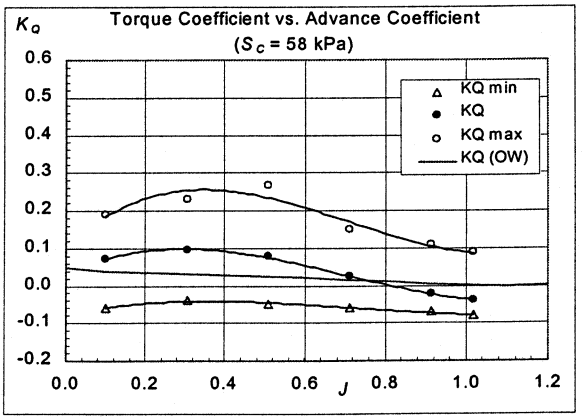

(b)

Figure 7. K_T and K_Q versus J for the *R-Class* propeller (S_C = 58 kPa).

4.2 Variation in ice strength

The effects of ice strength on loads are shown in Figures 8 and 9, where test results at three different ice strengths, 91kPa, 66kPa, and 58kPa, are compared. The cut depth was kept between 24mm to 25mm and the same range of J was investigated at each strength. Mean K_T and K_Q for each test series are shown in Figure 8.

The maximum and minimum K_T and K_Q are plotted in Figure 9. In Figure 9(a), the highest absolute values of thrust loads are the positive loads for $J < 0.6$ and the negative loads for $J > 0.6$. Overall, the worst loads are the backward loads at high values of advance coefficient. The highest absolute values of torque loads occur near $J = 0.4$ and are the positive acting loads.

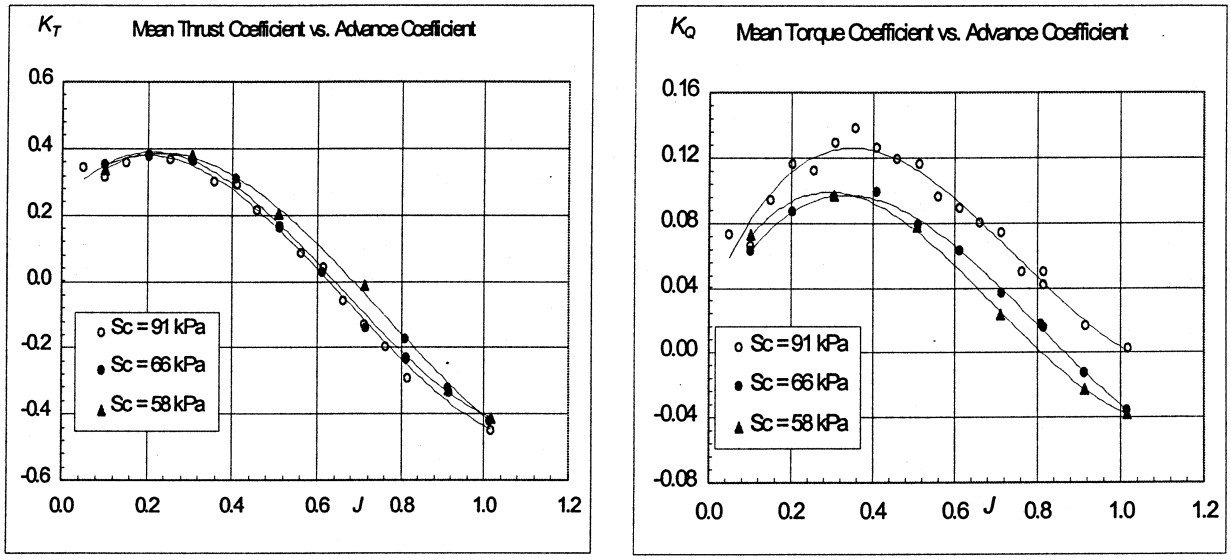

(a) (b)

Figure 8. Mean K_T and K_Q versus J (ice strength effects).

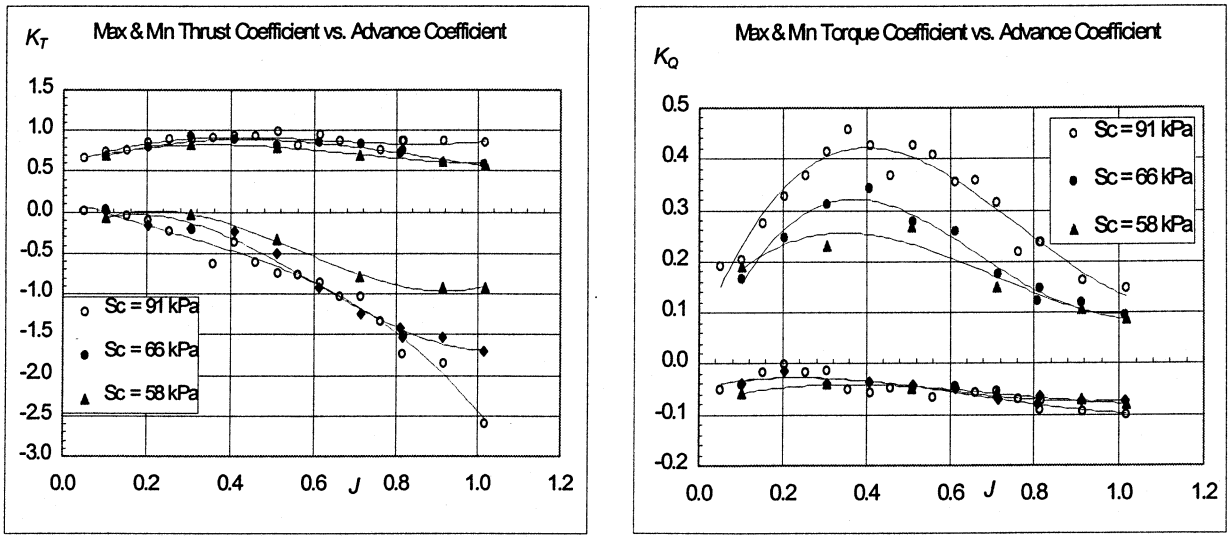

(a) (b)

Figure 9. Max K_T and K_Q versus J (ice strength effects).

The effect of strength is not uniform for the different loads. Ice strength had apparently little effect on the mean and maximum K_T, and minimum K_Q. Ice strength had significantly more effect on the mean and maximum K_Q, and some effect on the minimum K_T. Similar results have been found by Tamura and Yamaguchi (1997) in an experimental study of propeller load components. They found that the ice contact force was strongly dependent on ice strength and dominated the torque load, but that thrust loads were dominated by inertial forces, which they said were insensitive to ice strength.

The load data in Figures 8(a) and 8(b) are re-plotted in Figures 10a and 10b, which show the mean K_T and K_Q versus non-dimensional compressive ice strength, K_S, for different constant values of J, to illustrate further the influence of ice strength on the mean loads. As illustrated in Figure 10(a), variations in compressive ice strength index have minimal effect on the thrust coefficient over the entire range of J tested. Figure 10(b) shows that the torque coefficient is almost linearly related to changes in compressive ice strength index, and this relationship is consistent over the advance coefficient range $0.3 \leq J \leq 1.0$.

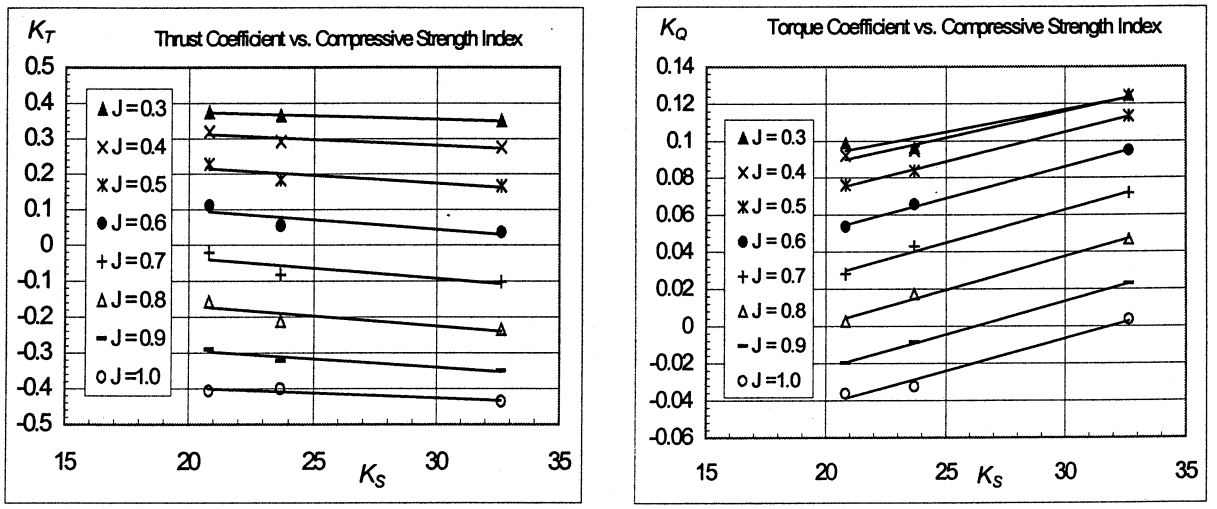

Figure 10. Mean K_T and K_Q versus K_S for values of J.

The average slopes of the K_T and K_Q versus K_S lines in Figure 10 are -0.00421 and 0.00327, respectively. It is possible to estimate K_T and K_Q for other values of K_S within the test range by interpolation. For this propeller, prediction of full-scale thrust and torque coefficients can be made using equations (6) and (7). Alternatively, predictions for each value of J can be made using the corresponding slope of the line, rather than the mean slope. The subscripts *FS* and *MS* denote full-scale and model-scale.

$$Mean: K_{T(FS)} = -4.21x10^{-3} \cdot (K_{S(FS)} - K_{S(MS)}) + K_{T(MS)} \tag{6}$$

$$Mean: K_{Q(FS)} = 3.27x10^{-3} \cdot (K_{S(FS)} - K_{S(MS)}) + K_{Q(MS)} \tag{7}$$

For example, the *R-Class* propeller has a diameter of 4.12m and operates at 2rps. Given a geometrically similar interaction of $h_I/D = 0.125$, a full-scale ice strength of 1.875MPa (which corresponds to 91kPa at model-scale) and ice density of 900kg/m^3, K_S is 30.7. Interpolation using the experimental data yields full-scale K_T and K_Q values for a range of advance coefficients, which are presented in Figure 11 as solid triangles. The experimental K_T and K_Q for model ice at 91kPa are also shown. As expected, the full-scale extrapolations have a similar form to the model results on which they are based. If these relationships hold over a wider range of K_S than that tested, then it should be possible to extrapolate K_T and K_Q for other values of K_S.

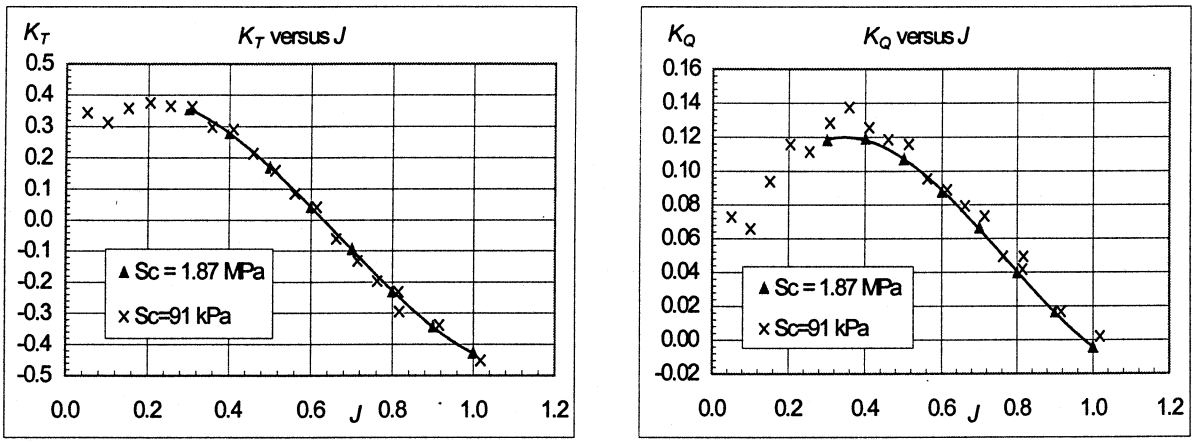

(a) (b)

Figure 11. Experimental and scaled mean K_T and K_Q versus K_S for values of J.

It is premature at this stage to propose this as a general method for making full-scale predictions of propeller performance in ice; rather it is an observation from a limited series of experiments. The observations showed regular behavior of ice loads with ice strength at a cut depth ratio of $h_I/D = 0.125$ and at a single shaft speed. It would be useful to investigate the effects of changes in shaft speed and cut depth ratio, and to test at higher ice strengths.

5. CONCLUSIONS

Results from a series of model propeller-ice interaction tests in an ice tank have been reported. Tests were done with an icebreaker propeller model at different ice strengths and over a range of operating conditions.

Results showed that, for this propeller, the highest overall thrust loads occur at high advance coefficients and tend to bend the blade aft. Such conditions might be limited to short term transitional operations in practice. The highest overall torque loads occurred at an advance coefficient of about 0.4. The ice contact force in this condition is such that the maximum thrust load is positive. Comparison of the mean thrust coefficient in ice with the corresponding open water performance curve indicated that the ice contact force acts primarily on the pressure side of the blade at low advance coefficients, and on the suction side at high advance coefficients. At all advance coefficients, the loads oscillate from positive to negative, which supports the requirement to design the blades against fatigue resulting from the ice induced loading.

Changes in the compressive strength of model ice were found to have relatively little effect on the mean and maximum values of thrust. Changes to ice strength resulted in an almost proportional change in the mean and maximum torque load. A closer look at the mean thrust and torque loads showed regular behavior of these loads with ice strength over a wide range of advance coefficient. This result was used to predict thrust and torque coefficients for the full-scale propeller. The prediction method is valid for the propeller studied and it is recommended that further work be done to assess its validity for this and other propellers over wider ranges of variations in ice strength, depths of cut, and propeller speeds.

ACKNOWLEDGMENTS

The work was funded primarily by the National Research Council Canada and the Natural Sciences and Engineering Research Council (Canada) through an NRC/NSERC program together with industry funding and support from Lloyd's Register of Shipping, Marineering Ltd. and KaMeWa. A special thanks to IMD for the use of their facilities and in particular the Ice Tank crew for their assistance in conducting the experiments. The authors are grateful for the thoughtful comments of the reviewers.

REFERENCES

Bose, N., Veitch, B. and Doucet, J.M. 1998. A design approach for ice class propellers. To appear, *SNAME Trans.*, Vol.106.

Doucet, J.M. 1996. Cavitation erosion experiments in blocked flow with two ice-class propeller models. *Master of Engineering Thesis*, Memorial University of Newfoundland.

Jones, S.J. 1993. Ice tank test procedures at the Institute for Marine Dynamics. *Report LM-AVR-20 (Revised)*, Institute for Marine Dynamics.

Katzmann, F.M. and Andriushin, A.V. 1997. Strength rates for blades as intended for the propellers of ice-breakers and ice ships. Russian Maritime Register of Shipping.

Searle, S. 1999. Ice tank tests of a highly skewed propeller and a conventional ice-class propeller in four quadrants. *Master of Engineering Thesis*, Memorial University of Newfoundland.

Searle, S., Veitch, B. and Bose, N. 1999. Experimental investigation of a highly skewed propeller in ice. To appear, *Proc. OMAE.*

Soininen, H., Jussila, M., Koskinen, P., Jones, S.J., Newbury, S. and Browne, R. 1997. Propeller-ice interaction. *SNAME Trans.*, Vol. 105.

Tamura, K. and Yamaguchi, H. 1997. Experimental study to separate into components the interaction force between propeller and ice piece. *INSROP Working Paper*, No.87, I.1.9, International Northern Sea Route Programme.

Timco, G.W. 1986. EG/AD/S: A new type of model ice for refrigerated towing tanks. *Cold Regions Science and Technology*, Vol.12, No.2: 175-195.

Walker, D.L.N. 1996. The influence of blockage and cavitation on the hydrodynamic performance of ice class propellers in blocked flow. *Doctoral Thesis*, Memorial University of Newfoundland.